Experimental study of plane wave propagation in a corrugated pipe: Linear regime of acoustic-flow interaction

Joachim Golliard, Yves Aurégan, Thomas Humbert

Experimental study of plane wave propagation in a corrugated pipe: linear regime of acoustic-flow interaction

Joachim Golliard[a,b,*], Yves Aurégan[b], Thomas Humbert[b]

[a] *Centre de Transfert de Technologie du Mans (CTTM), 20 rue Thalès de Milet, 72000 Le Mans, France*
[b] *Laboratoire d'Acoustique de l'Université du Mans (LAUM), Avenue Olivier Messiaen, 72085 Le Mans Cedex 9, France*

Abstract

Acoustic propagation in corrugated pipes offers interesting features in presence of a mean flow, which are investigated experimentally in this paper. The scattering matrix of the corrugated section is measured with and without a mean flow. The analysis of the results is based on the extraction of the wavenumbers of propagation within the corrugated pipe. Without flow, a small decrease of the speed of sound and a slight increase of the attenuation are observed. In presence of mean flow, oscillations against the frequency of both the real part and the imaginary part of the wavenumber occur. For sufficiently large flow velocities, the oscillation caused by the sound-flow interaction is such that the acoustic waves are amplified by the flow. The Strouhal number for maximum gain shows a small dependency on the Reynolds number, and converges to values of 0.4 to 0.5 depending on the presence of rounded or sharp upstream edges of the cavities. Nonlinear effects begin to appear for an acoustic amplitude such that the acoustic velocity is about 1% of the flow velocity.

Keywords: Aeroacoustics, Corrugated pipes, Duct acoustics, Hydrodynamic mode, Scattering

*Corresponding author

Email addresses: jgolliard@cttm-lemans.com (Joachim Golliard), yves.auregan@univ-lemans.fr (Yves Aurégan), thomas.humbert@univ-lemans.fr (Thomas Humbert)

1. Introduction

Corrugated pipes are found in various industrial applications, where a global flexibility is required (to allow some relative movement of the two ends of the pipe) while a local strength is also needed (for example to contain the flow and to resist to high inner and/or outer pressures). Typical applications are hoses for vacuum cleaners or ventilation, flexible tubing used for cooling of high-end equipment, or multi-layered flexible pipes used for transport of natural gas between installations and export pipe lines on an offshore platform. The different designs involved (below-type flexible pipes or folded and interlocked thin plate) all have an inner wall surface presenting some axis-symmetrical (or nearly axis-symmetrical) cavities. In cases where it is not possible to add a smooth liner as innermost layer, the flow of gas or liquid through the pipe can lead to the generation of acoustic tones.

The phenomenon of "whistling pipes" was first reported as early as 1922 by Burstyn [1] and Cermak [2, 3]. In the following years, a number of studies have been published, providing further empirical and theoretical understanding of this problem [4, 5, 6, 7]. The motivation for these studies was often scientific curiosity, but could also be for musical purposes [8, 9, 10] or industrial applications. Indeed, flow-induced pulsations in corrugated pipes can lead to serious industrial problems [11] or discomfort for users of domestic appliances.

Most studies have been considering the self-induced oscillation mechanism leading to the whistling. An interesting approach to determine if whistling is possible at a given flow velocity is based on a power balance analysis [7]. In this approach, illustrated in Figure 1, it is considered a necessary condition for whistling that the acoustic power generated by the cavities balances the acoustic power dissipated anywhere in the system. The generated acoustic power can be evaluated numerically [7, 12] or experimentally [13, 14, 15] and even extrapolated to other cases with empirical rules [16]. These approaches allow the estimation of the onset velocity of a particular pipe in a particular environment and the amplitude and frequency of the tones can be evaluated, within a certain confidence. Nevertheless, except for [17, 18, 19] the studies were performed under conditions of whistling or at least quasi-whistling, i.e. in the non-linear regime.

In a complementary way, we focus in this paper on the linear regime for which no whistling can occur. Obviously, this type of study does not make it possible to predict the amplitude of the whistling but gives precise criteria for

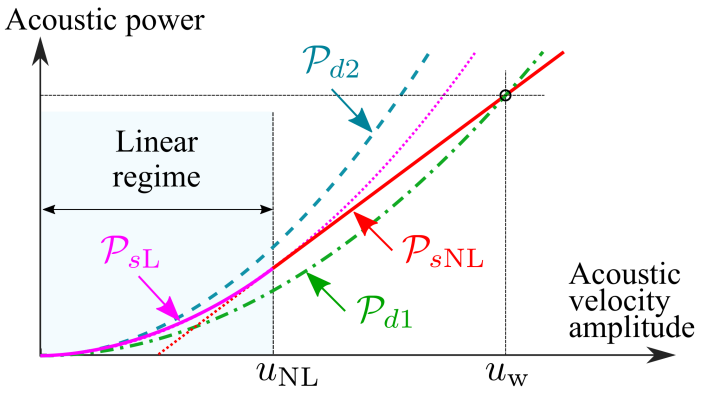

Figure 1: (Color online) Schematic illustration of the balance between power production and dissipation in a corrugated pipe: The acoustic power provided by the corrugated pipe increases quadratically with the sound level, $\mathcal{P}_{s\mathrm{L}}$, for a level $u < u_{\mathrm{NL}}$ then increases along a straight line ($\mathcal{P}_{s\mathrm{NL}}$ for an acoustic velocity amplitude $u > u_{\mathrm{NL}}$). Two linear dissipative cases are represented (the dissipated power increases quadratically). In the first case, $\mathcal{P}_{d1}$, the dissipated power is less than the produced power at low level and an equilibrium can occur in the non-linear region for $u = u_{\mathrm{w}}$ which results in a stable whistling. In the second case, $\mathcal{P}_{d2}$, the dissipated power is always larger than the produced power and no whistling can exist.

its onset. This linearity of phenomena makes it possible to use classical tools such as the scattering matrix of a corrugated pipe section. From the scattering matrix of a corrugated section, the dissipation or amplification of energy can be determined [20]. This approach, based on experimental identification of the scattering matrices, was used to study the potentiality of whistling of an orifice with flow [21, 22] and the $\mathcal{PT}$ (parity-time) symmetrical behavior of two orifices mounted in tandem, one providing absorption and the other one amplification [23]. The method has also been extended to the study of multiports such as T-junctions [24].

The present study reports an experimental investigation of linear acoustic propagation in a pipe with corrugated walls in presence of mean flow. In section 2, the experimental setup, the geometry of the tested pipe, and the measurement procedure are described. The result of this step is the scattering matrix of the corrugated pipe, without flow or with flow. This allows to quantify the effect of the flow on the reflection and transmission coefficients. In section 3, the wavenumber of the sound waves propagating in the corrugated pipe are extracted from the scattering matrix. In presence of flow, the imaginary part of the wavenumber becomes positive, indicating

an amplification of sound waves. In last section, a discussion of the results is provided. Particularly, a gain-due-to-flow coefficient is defined as the difference between the amplification coefficient with flow and the amplification coefficient without flow. The dependence of the maximum for this gain (and of the Strouhal number at which it is maximum) on parameters such as the amplitude and the Mach number allows to separate the different effects of the flow.

2. Measuring acoustic propagation in a corrugated pipe

The present investigation is based on the measurement of the scattering matrix of a corrugated pipe subjected to a mean flow. By definition, the scattering matrix linearly connects the outgoing waves to the incident waves. Therefore, measurements are made in the linear regime, under conditions where no whistling occurs. The experimental setup allowing this measurement is described in Section 2.1. The description of the experiments, as well as some results illustrating typical coefficients of the scattering matrix without flow and in presence of a mean flow through the pipe, are provided in Section 2.2.

2.1. Experimental setup

The investigated corrugated tube is shown in Figure 2(a). It is composed of 165 elements with a pitch equal to 12 mm (total length of the tube: L_1 = 165×12 = 1980 mm). The elements are screwed together and the sealing is achieved by O-rings. Some measurements are also performed on the same tube but with only 103 elements, leading to a total length L_2 = 1236 mm. Each element is the same with a plateau of length $l_p = 8$ mm and a cavity of width $l_c = 4$ mm. The inner radius $R_p = 15$ mm at the plateaus corresponds to the inner radius of the smooth pipes in the experimental setup. The larger radius $R_c = 19$ mm creates cavities of depth 4 mm. The cavities have a square shape (4 mm × 4 mm) but the edges of the cavities are not symmetrical. Most measurements reported in this paper are done in the configuration *SR*, illustrated in Figure 2(a), where the upstream edges of the cavities are sharp while the downstream edges are rounded (radius r = 1 mm). The inverted configuration is called *RS*.

The corrugated tube is mounted in a flow-rig between two measurement sections (see Figure 2(b)). A mean flow is provided by a centrifugal fan, and the flow rate can be continuously varied in order to provide a mean flow

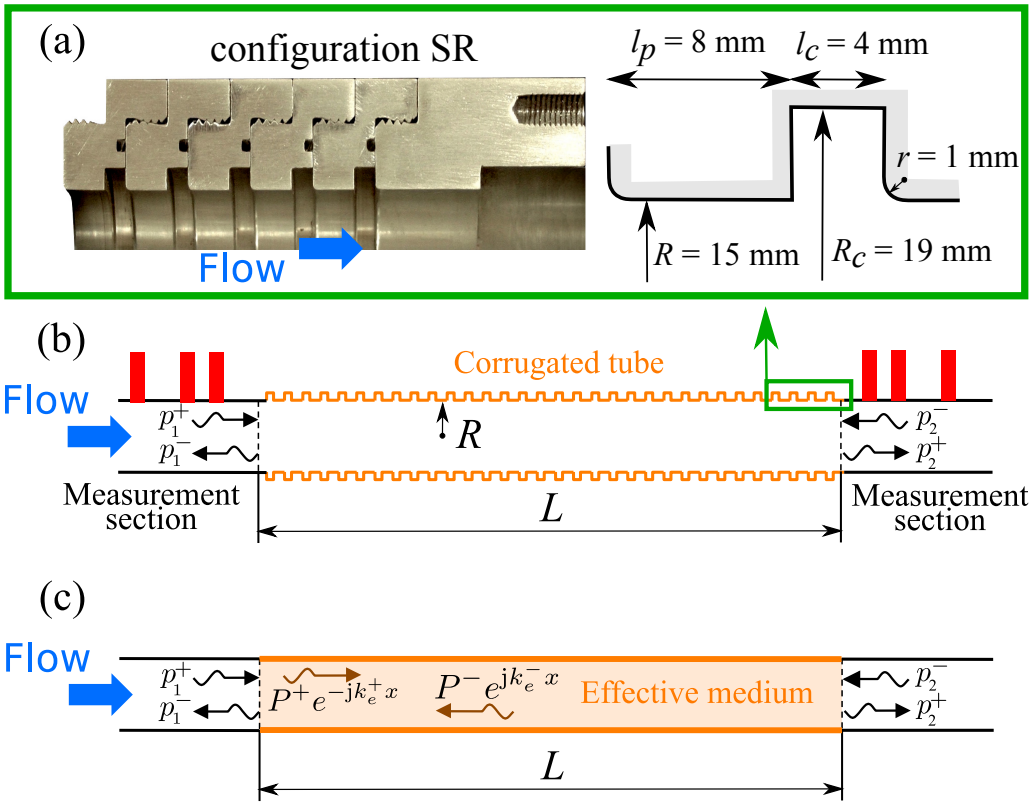

Figure 2: (Color online) (a) Picture of a cut of the elements composing the corrugated tube (left), sketch and dimensions of a cavity of the corrugated tube (right). The arrow indicating the flow here corresponds to configuration *SR*. (b) Sketch of the experimental setup with the corrugated tube subjected to a mean flow and placed between measuring sections equipped with microphones. (c) Drawing of the setup where the corrugated tube is modeled as a tube filled with an equivalent medium.

velocity up to 20 m/s in the corrugated tube. The mean-flow velocity U_0 is measured in two different ways depending on the range of flow rates. At low flow rates, it is determined from the measurement of the pressure drop over a calibrated resistance. At higher flow rates, it is measured with a turbine flow meter. The Mach number is defined by $M = U_0/c_0$ where c_0 is the speed of sound in the gas.

Each of the measurement sections consists in a hard walled steel duct of radius R = 15 mm where four 1/4-in microphones (B&K 4136 with Nexus 2690 amplifier) are mounted. A relative calibration of the microphones was performed in-situ to avoid disassembling them from their supports (see Figure

2 of [25]). The distances between the four microphones are respectively 30 mm, 145 mm and 288 mm (either upstream or downstream of the sample). An overdetermined measurement of the incoming and outgoing waves can thus be performed on both sides of the measured system from 100 Hz to 4000 Hz in steps of 5 Hz. In this frequency range, only plane waves propagate. The over-determination of the system to be solved is used to adjust the speed of sound by an optimization process.

Two acoustic sources, mounted on both sides of the system, give for each frequency two different acoustic states, and the four elements of the scattering matrix (transmission and reflection coefficients in both directions) for plane waves can be evaluated for the corrugated pipe as a whole. A more detailed description of the measurement technique and of the facility can be found in [25].

The signal acquisition was performed by a National Instrument acquisition system (NI cDAQ-9178 + 7 × NI 9234 + NI CRIO-9263) driven by an in-house acquisition software called *INTAC*. This acquisition system is used in the sine sweep mode and an average over 300 cycles is used at each frequency step. In this study, particular attention is devoted to stay in the linear regime of the sound-flow interactions happening in the corrugated tube. A first step for this purpose is ensuring that the incident waves have a controlled amplitude. Therefore, a specific controller has been included in *INTAC* to ensure a constant amplitude of the incident acoustic wave. To that end, a first measurement is made with a constant source level and the recorded pressure field is decomposed in terms of the two possible directions of propagation of the acoustic plane waves. The measurement is made again with a source level such that the incident level is equal to a pre-determined value. This process is repeated until the amplitude of the incident acoustic wave is within 2% of the predetermined level. It has then been verified that the coefficients of the scattering matrix are independent on the amplitude of the incident field. In the case without flow, the propagation remains linear up to an amplitude of 120 dB.

By performing two measurements, one with the upstream source on (downstream side with low reflections), one with the downstream source on (upstream side with low reflections), the scattering matrix $\mathbf{S}$ of the corrugated tube is finally computed:

$$\begin{pmatrix} p_2^+ \\ p_1^- \end{pmatrix} = \mathbf{S} \begin{pmatrix} p_1^+ \\ p_2^- \end{pmatrix} = \begin{bmatrix} T^+ & R^- \\ R^+ & T^- \end{bmatrix} \begin{pmatrix} p_1^+ \\ p_2^- \end{pmatrix}, \tag{1}$$

with $p_i^{\pm}$ the amplitude of the forward- and backward-propagating plane waves, where $i = 1$ defines the position upstream, and $i = 2$ the position downstream of the corrugated pipe.

2.2. Effect of flow on the transmission coefficient

Figure 3 displays the magnitudes of the transmission coefficients measured for a corrugated pipe of length $L_1 = 1980$ mm without flow and with a mean flow at $M = 0.01$, $M = 0.016$ and $M = 0.029$ in configuration SR (with upstream cavity edges sharp and downstream cavity edges rounded with 1 mm).

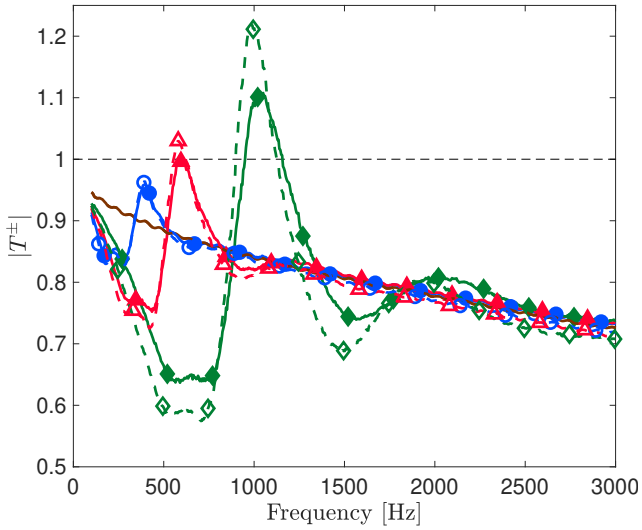

Figure 3: (Color online) Transmission coefficients as a function of the frequency.
T^+: (M= 0), (M= 0.01), (M= 0.016), (M= 0.029);
T^-: (M= 0), (M= 0.01), (M= 0.016), (M= 0.029).
Note: The symbols are here to distinguish the different measurement series. In no case they indicate the data points, as the frequency spacing of the measurements is 5 Hz. This also applies to Figures 4 to 7.

Without flow, the transmission coefficients T^+ and T^- are equal as a result of the reciprocity. The difference between $|T^{\pm}|$ and 1 is due to the visco-thermal losses along the corrugated pipe. The small oscillations which can be observed are due to small reflections at the interfaces between the corrugated tube and the smooth tube, since the effective speed of sound and the characteristic impedance slightly differs from one tube to the other.

With flow, large oscillations of the modulus of the transmission coefficients are observed. At low frequencies, transmission coefficients are lower with flow compared to the no-flow case. This indicates that the flow produces additional absorption in this frequency range. Then, over a finite frequency range, the transmission coefficients with flow increase and become higher than the no-flow case, indicating that the flow causes some amplification. A few additional zones of absorption and amplification, compared to the no-flow case, are observed at higher frequencies, but the oscillations are damped at high frequencies and the curves tend towards the no-flow curve. It is interesting to note that above a certain velocity ($M = 0.016$ in the present case) the transmission coefficient can become greater than 1. It means that amplification due to the flow is larger than the absorption due to visco-thermal losses: the sound waves are overall amplified for a limited frequency range as they pass through the corrugated tube.

The equality of $|T^+|$ and $|T^-|$ that existed without flow is destroyed by the flow. Part of this phenomenon is caused by the convection which very slightly increases T^+ and decreases T^- for the measured Mach numbers, but the largest effect is that the oscillations due to the flow are significantly larger for T^- than for T^+, with a small shift in frequency. These two different effects will be isolated from each other by the extraction of the effective propagation wavenumber in the next section.

3. Wavenumbers deduced from the scattering matrix

3.1. The corrugated tube as an effective medium

In this section, the propagation in the corrugated tube is described by an effective medium. A simple way for that is to consider the transfer matrix $\mathbf{T}$ linking the downstream waves (p_2^+ and p_2^-) to the upstream waves (p_1^+ and p_1^-):

$$\begin{pmatrix} p_2^+ \\ p_2^- \end{pmatrix} = \begin{bmatrix} T_{11} & T_{12} \\ T_{21} & T_{22} \end{bmatrix} \begin{pmatrix} p_1^+ \\ p_1^- \end{pmatrix}. \tag{2}$$

The coefficients of this transfer matrix can be easily computed from the coefficients of the scattering matrix by

$$T_{11} = T^+ - R^+R^-/T^-, \qquad T_{12} = R^-/T^-,$$
$$T_{21} = -R^+/T^-, \qquad T_{22} = 1/T^-.$$

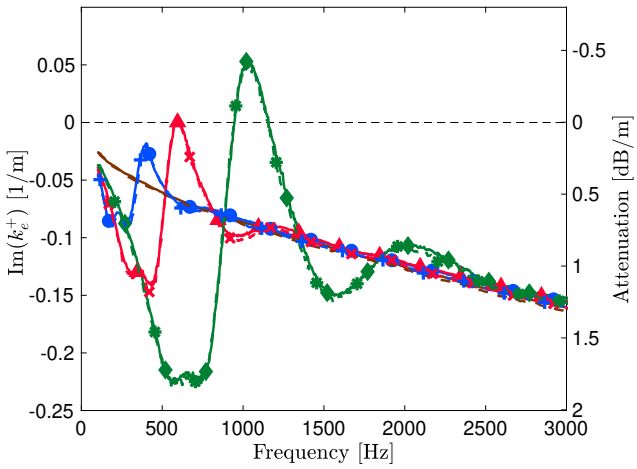

Figure 4: (Color online) Imaginary part of the effective wavenumbers k_e^+ as a function of the frequency for the two tubes of different lengths.
L_1 = 1950 mm: —(M= 0), —●—(M= 0.01), —▲—(M= 0.016), —◆—(M= 0.029);
L_2 = 1236 mm: - - -(M= 0), - - + - -(M= 0.01), - - × - -(M= 0.016), - - ✱ - -(M= 0.029).

The transfer matrix can also be decomposed in

$$\mathbf{T} = \mathbf{V}\,\mathbf{E}\,\mathbf{V}^{-1}, \tag{3}$$

where $\mathbf{E}$ is the diagonal matrix composed of the eigenvalues E^+ and E^- of $\mathbf{T}$, and $\mathbf{V}$ is a matrix whose columns are the corresponding eigenvectors. It can be noted that each of the two eigenvectors is defined by only one parameter (noted here Z_e^+ and Z_e^-) and that these eigenvectors can be normalized so that the following relationships can be written:

$$\begin{aligned} p_1^+ + p_1^- &= P^+ + P^-, & p_2^+ + p_2^- &= P^+E^+ + P^-E^-, \\ p_1^+ - p_1^- &= Z_e^+P^+ - Z_e^-P^-, & p_2^+ - p_2^- &= Z_e^+P^+E^+ - Z_e^-P^-E^-, \end{aligned} \tag{4}$$

leading to

$$\mathbf{V}^{-1} = \frac{1}{Z_e^+ + Z_e^-}\begin{bmatrix} 1+Z_e^- & -1+Z_e^- \\ -1+Z_e^+ & 1+Z_e^+ \end{bmatrix}, \mathbf{V} = \frac{1}{2}\begin{bmatrix} 1+Z_e^+ & 1-Z_e^- \\ 1-Z_e^+ & 1+Z_e^- \end{bmatrix}. \tag{5}$$

The four parameters E^+, E^-, Z_e^+ and Z_e^- can be computed from the measured scattering matrix. To go a step further, we now consider that $E^\pm$ represent the propagation of forward-traveling and backward-traveling

waves in the corrugated pipe, thus assuming that $E^+ = \exp(-\mathrm{j}k_e^+ L)$ and $E^- = \exp(-\mathrm{j}k_e^- L)$. A specific measurement has been performed to validate this assumption: The scattering matrices of two tubes of different lengths ($L_1 = 165\times12 = 1980$ mm and $L_2 = 103\times12 = 1236$ mm) have been measured and the parameters Z_e^+ and Z_e^- deduced from these two series of measurements have been compared, as well as the two effective wavenumbers k_e^+ and k_e^-. The effective parameters $Z_e^\pm$ and $k_e^\pm$ appear to be equal when computed from the measurements in the two pipes of different lengths, as illustrated by Figure 4 showing a comparison of the imaginary part of the effective wavenumbers k_e^+.

The corrugated tube can thus be described as a one-dimensional effective medium where the effective wavenumbers k_e^+ and k_e^- can be computed from the experimental scattering matrix. The matching conditions at both ends of the tube are given by Eqs. (4) where the parameters Z_e^+ and Z_e^- are also deduced from the experiments.

3.2. Measured acoustic wavenumbers in a corrugated pipe with flow

The real part of the wavenumber leads to an effective speed of sound $c_e^\pm = \omega/k_e^\pm$, where $\omega = 2\pi f$, with f the frequency. This effective speed of sound $c_e^\pm$ is plotted in Figure 5 after being normalized by c_0 and corrected from the convective effects.

The speed of sound without flow (line without symbol) is about 92% of what it would be without corrugations. This is a classical effect of slowing down of the acoustic waves when the wall of a tube is lined with cavities[26]. A first approximation of the decrease in wave speed is given by the square root of the ratio between the volume of the tube without corrugations and the volume of the tube with corrugations. It leads to a good agreement with the measurements:

$$\sqrt{(l_p + l_c)/(l_p + l_c R_c^2/R^2)} = 0.91. \tag{6}$$

The convection induces an increase or a decrease of the effective speed of sound with a factor $(1 \pm M)$, as for propagation in smooth pipes. This effect is displayed in the inset of Figure 5 showing c_e/c_0, where it is clear that c_e measured in the flow direction (plain lines) increases for increasing Mach number while c_e measured in the direction opposite to the flow (dashed lines) decreases. When the speed of sound is divided by $1 \pm M$, as in the main figure, all the curves tend to collapse.

Nevertheless, after the correction for the convective effects, a difference can still be observed between the curves corresponding to the measurements

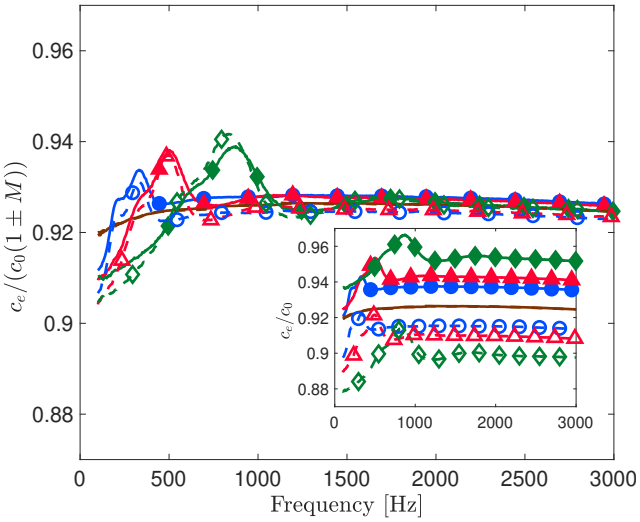

Figure 5: (Color online) Relative effective wave speed c_e/c_0 in the corrugated tube in configuration *SR*, as a function of the frequency (inset) and divided (main figure) by 1+M (forward propagation) or 1−M (backward propagation).
Forward propagation: (M= 0), (M= 0.01), (M= 0.016), (M= 0.027);
Backward propagation: (M= 0), (M= 0.01), (M= 0.016), (M= 0.027).

with flow and without flow: a small oscillation in the speed of sound can be seen. The frequency at which these oscillations occur increase linearly with flow velocity.

The imaginary part of the wavenumber is related to the amplification coefficient of the propagating waves. In Figure 6, this amplification coefficient, $\mathrm{Im}(k_e^+)$ for forward-propagating waves and $-\mathrm{Im}(k_e^-)$ for backward-propagating waves, is plotted versus frequency at different flow velocities. In general, the amplification coefficient is slightly negative because it reflects the damping of the acoustic waves, mainly due to visco-thermal losses at the pipe walls. This is indeed what is observed here for the case without flow (lines without symbols). In this case, the attenuation without flow is about 40% larger than what it would be in a smooth pipe of identical inner diameter. However, in presence of flow, a frequency-dependent oscillation is observed around the no-flow curve. This means that the flow acts as an amplifier for the acoustic wave at certain frequencies and as a damper at other frequencies. The oscillations are actually so large that the total amplification coefficient becomes positive if the velocity is large enough. For the case illustrated in Figure 6, this occurs when the Mach number is larger than

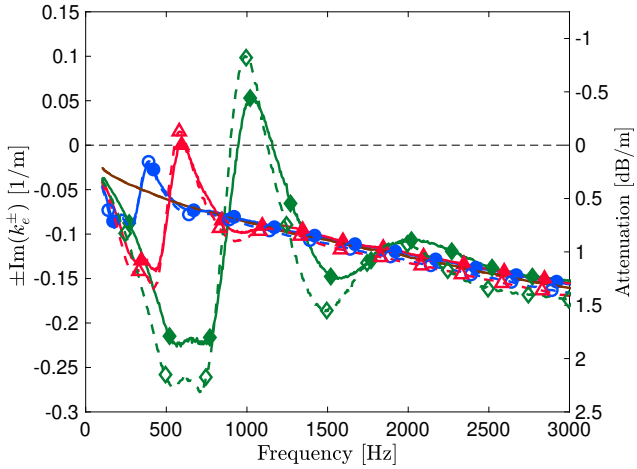

Figure 6: (Color online) Imaginary part of the effective wavenumbers as a function of the frequency in the corrugated tube in configuration *SR*.
k_e^+: (M= 0), (M= 0.01), (M= 0.016), (M= 0.027);
$-k_e^-$: (M= 0), (M= 0.01), (M= 0.016), (M= 0.027).

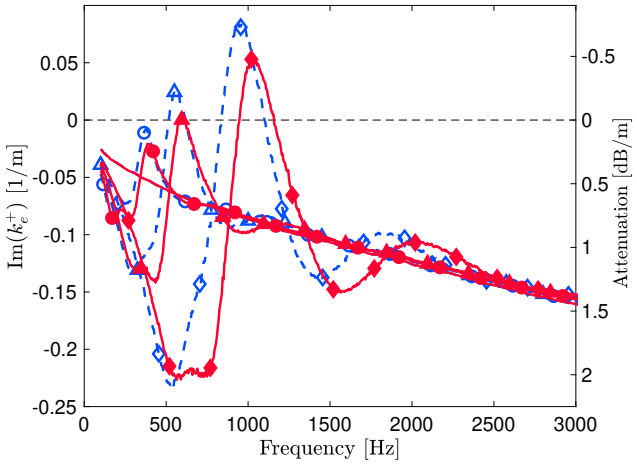

Figure 7: (Color online) Imaginary part of the effective wavenumbers k_e^+ as a function of the frequency for the two flow directions.
Configuration *RS*: (M= 0), (M= 0.010), (M= 0.016), (M= 0.027);
Configuration *SR*: (M= 0), (M= 0.010), (M= 0.016), (M= 0.027).

0.016. As with the real part of the effective wavenumbers, the frequencies at which these oscillations occur are nearly linearly dependent on the flow velocity, suggesting maximum gain for a nearly constant Strouhal number.

The corrugated pipe used for the tests is not symmetrical, as displayed in Figure 2(a). All the results reported above correspond to configuration *SR*, where the cavities have a sharp upstream edge and a rounded downstream edge. In Figure 7, wavenumbers measured for both flow directions are compared. For configuration *RS*, the amplitude of the oscillations is slightly larger and the frequency of the peak of amplification is lower than for configuration *SR* at the same velocity. This agrees with earlier studies on whistling corrugated pipes [11, 6], where it was observed that an asymmetrical pipe would whistle at a lower threshold velocity (or onset velocity), and with a slightly lower frequency, when installed with upstream rounded edges. Indeed, an oscillation of larger amplification (as is the case reported here for configuration *SR* compared to configuration *RS*) means that absolute amplification of the sound waves occurs at a lower velocity. Furthermore, Belfroid et al. [11, 6] explain the lower whistling frequency for configuration *SR* by the fact that vortex shedding can occur at the start of the rounding of the upstream edge, imposing a longer path for free vorticity.

4. Discussion

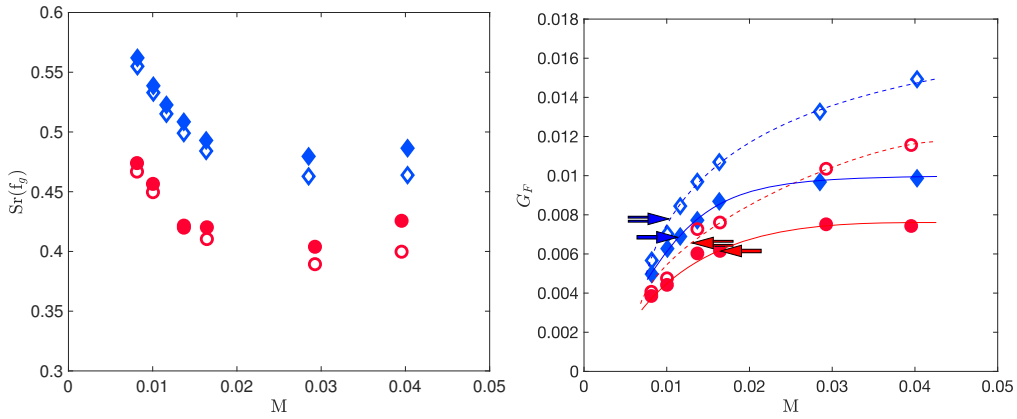

Figure 8: (Color online) (a) Strouhal number at the maximum of the amplification coefficient as a function of the Mach number. (b) Gain-due-to-flow coefficient G_F as function of the Mach number. Configuration *SR*: ● (Forward traveling waves), ○ (Backward traveling waves), Configuration *RS*: ◆ (Forward traveling waves), ◇ (Backward traveling waves). (b): The arrows mark, for each case, the minimum Mach number at which the sound wave becomes amplified.

In Figure 8(a), the Strouhal number ($Sr = f_g l_c / U_0$) corresponding to the

frequency f_g for which the maximum of amplification occurs, is plotted versus the Mach number for the two flow directions. By definition, the Strouhal number would be constant if the frequency f_g was linearly dependent on the flow velocity U_0. Actually, this frequency deviates from a linear dependence when the flow velocity is very low (20% increase at $M = 0.008$ compared to the asymptotic value obtained when $M > 0.02$). At such low flow velocities (corresponding to Reynolds numbers of less than $2{\cdot}10^5$), the pipe flow is possibly not completely developed and the profile of flow velocity becomes less flat [27]. The effective boundary-layer thickness increases, and thus the convection velocity in the shear layers above the cavities decreases, leading to an increase of the Strouhal number. A similar increase of the Strouhal number for increasing boundary-layer thickness has been observed by Kooijman et al. [28] for sound amplification at orifices. Similarly, the effect of larger diameter on the peak-whistling Strouhal number in the case of whistling corrugated pipes is explained as due to the increasing effective boundary-layer thickness (or confinement ratio of the cavities) in [7].

As noted in the preceding section, the orientation of the cavities related to the flow direction has a significant impact on the amplification peak and thus on the Strouhal number: For the flow configuration *RS*, the Strouhal number tends to 0.47, while it tends towards a lower value of 0.42 for the configuration *SR*. This can partly be explained by the fact that the rounding edge increases the effective path of free vorticity [11, 6]. Note that the Strouhal number is defined here from the cavity width l_c and not from the cavity width augmented by the radius upstream edge $l_c + r$. For each configuration, the Strouhal number is also slightly larger for forward-traveling waves than for backwards-traveling waves.

A gain-due-to-flow coefficient is defined as the difference between the normalized amplification coefficient measured with flow (taken at the frequency f_g where the strongest amplification due to the flow occurs) and the normalized amplification coefficient measured without flow (taken at the same frequency f_g): $G_F = \mathrm{Im}(k_e^+/k_0)_M - \mathrm{Im}(k_e^+/k_0)_{M=0}$ for forward-traveling waves and $G_F = -\mathrm{Im}(k_e^-/k_0)_M + \mathrm{Im}(k_e^-/k_0)_{M=0}$ for backward-traveling waves. This allows to separate two distinct effect: the visco-thermal losses at the walls of the pipe and the amplification/attenuation of acoustic waves due to the vortex-sound interaction. This flow gain G_F is plotted in Figure 8(b) versus the Mach number. The fact that the amplification due to the flow is more important for the configuration *RS* than for the opposite flow direction (configuration *SR*) is clearly demonstrated in this figure. Furthermore,

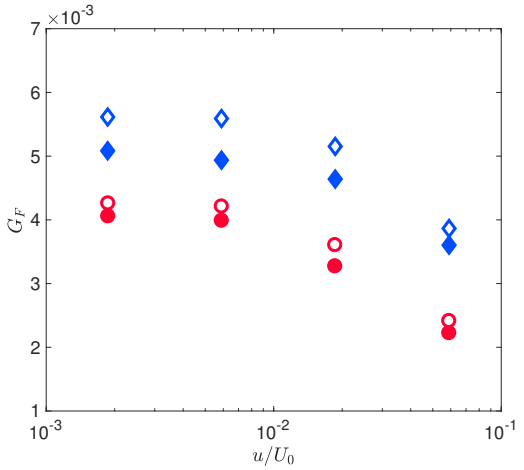

Figure 9: (Color online) Gain-due-to-flow coefficient G_F as a function of u/U_0 , for M= 0.008 and pipe length L_1. Configuration *SR*: ● (Forward traveling waves), ○ (Backward traveling waves), Configuration *RS*: ◆ (Forward traveling waves), ◇ (Backward traveling waves).

the influence of the direction of the acoustic waves (backward propagating or forward propagating) for a same configuration is also noticeable in this figure: waves traveling against the flow are more amplified than waves traveling in the same direction as the mean flow. For all configurations, the flow gain G_F increases linearly with the Mach number at low flows and then flattens out for increasing Mach numbers. This reduced growth when the Mach number increases is unexpected and calls for further investigations.

The incident wave level $|p_i^+|$ has been controlled and varied during the measurements. In Figure 9, the flow gain G_F is plotted as a function of this parameter. To facilitate the comparison with other available results [7, 11], the incident pressure level has been converted into a relative velocity u/U_0 by using $u = |p_i^+|/\rho_0 c_0$. The measurements in Fig. 9 have been performed at a single main-flow velocity (M = 0.008) for which the wave is always attenuated ($\pm\mathrm{Im}(k_e^{\pm}/k_0) < 0$). The results show that the flow gain is independent of the level when $u/U_0 < 1\%$. For larger values of u/U_0, the flow gain with the amplitude, as described by Nakiboğlu et al. [7]. It should be noted that since the gain varies with amplitude and the amplitude varies along the corrugated tube, the values of G_F are an average of all values along the tube (although, for this measurement, the level varies only slightly along the duct, the transmission coefficient being in the order of 0.94). Note also that all

the other measurements reported in the rest of this article correspond to amplitudes u/U_0 lower than 1%.

A surprising consequence of the decrease of G_F when the acoustic amplitude increases is illustrated in Fig. 10. If the flow Mach number is high enough ($M \approx 0.016$ for the present tube mounted in configuration SR), the flow gain G_F is larger than the thermo-viscous losses and $\mathrm{Im}(k_e^+)$ is positive. As G_F decreases with the level, there is a point where the gain and losses exactly compensate ($\mathrm{Im}(k_e^+) = 0$). If the incident pressure has an amplitude smaller than this value, the wave is amplified until it reaches the value for which $\mathrm{Im}(k_e^+) = 0$. On the contrary, if the incident pressure has a larger amplitude, the wave is damped. Therefore, for a sufficiently long corrugated tube with amplification, the output wave will have the same amplitude, regardless of the amplitude of the incident wave.

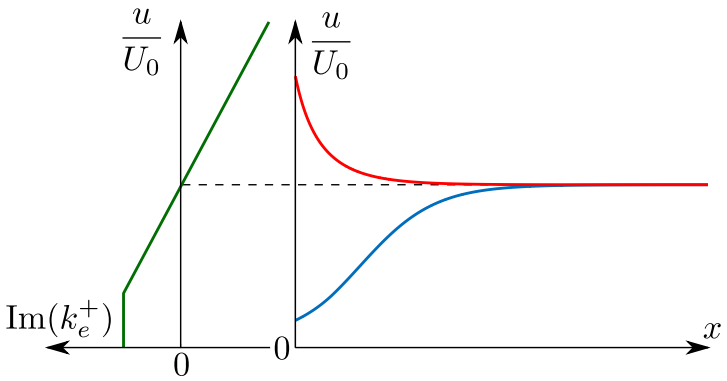

Figure 10: (Color online) Illustration of the saturation of the amplitude of a wave propagating along x when the flow gain G_F is going from positive (at small u/U_0) to negative. Left curve : amplification coefficient as a function of the relative velocity. Right plot: Spatial evolution of the relative velocity along the propagation axis when the initial value is above the threshold (Red curve) or below the threshold (Blue curve).

5. Conclusions

The acoustic propagation in a corrugated pipe without flow and in presence of mean flow has been measured. Without flow, the main effect of the corrugations is to slow down the acoustic waves and to increase their attenuation. In presence of mean flow, two effects are observed. First, as for smooth pipes, convection modifies the real part of the wavenumber. On the other hand, the flow creates an oscillation of the wavenumber (as a function of

frequency) around the wavenumber measured without flow. This oscillation is visible both on the real part and the imaginary part of the wavenumber. The oscillation of the imaginary part of the wavenumber reflects an additional gain (or attenuation) due to the sound-flow interaction. For sufficiently high velocities, the additional gain may be larger than the attenuation without flow, which means that the sound waves are linearly amplified by the flow as they travel in the corrugated pipe. This effect is more pronounced when the cavities have an upstream edge rounded than when their upstream edge is sharp.

The frequencies of the maximum gain due to the flow corresponds to Strouhal numbers of 0.4 or 0.5 depending on the direction-installation of the pipe. For the lowest flow velocities, the Strouhal number increases due to the thicker boundary layer at lower Reynolds numbers. On the other hand, at a constant Reynolds number, the gain decreases when the amplitude of the incident acoustic waves becomes larger than a threshold of about 1% of the main-flow velocity. These results confirm and refine earlier studies which were mainly performed with corrugated pipes in whistling (or nearly whistling) regime with standing waves. This also indicates that a linear analysis relying on scattering of propagating waves by the corrugated pipe is suitable to determine the threshold of whistling.

References

[1] W. Burstyn, Eine Neue Pfeife (A new pipe), Z. Tech. Phys. (Leipzig) 3 (1922) 179–180.

[2] P. Cermak, Über die Tonbildung bei Metallschläuchen mit Eingedrücktem Spiralgang (On the sound generation in flexible metal hoses with spiraling grooves), Phys. Z. 23 (1922) 394–397.

[3] P. Cermak, Über die Tonbildung in Luftdurch-Strömten Röhren (On the production of tone in an air-flows through tubes), Phys. Z. 25 (1924) 121–130.

[4] A. M. Binnie, Self-induced waves in a conduit with corrugated walls. ii. experiments with air in corrugated and finned tubes, Proc. R. Soc. London. Ser. A. Math. Phys. Sci. 262 (1309) (1961) 179–191.

[5] F. S. Crawford, Singing corrugated pipes, Am. J. Phys. 42 (4) (1974) 278–288.

[6] G. Nakiboğlu, S. P. Belfroid, J. F. Willems, A. Hirschberg, Whistling behavior of periodic systems: Corrugated pipes and multiple side branch system, Int. J. Mech. Sci. 52 (11) (2010) 1458–1470, special Issue on Non-linear Oscillations.

[7] G. Nakiboğlu, S. Belfroid, J. Golliard, A. Hirschberg, On the whistling of corrugated pipes: effect of pipe length and flow profile, J. Fluid Mech. 672 (2011) 78–108.

[8] M. P. Silverman, G. M. Cushman, Voice of the dragon: the rotating corrugated resonator, Eur. J. Phys. 10 (4) (1989) 298–304.

[9] S. Serafin, J. Kojs, Computer models and compositional applications of plastic corrugated tubes, Organised Sound 10 (1) (2005) 67–73.

[10] G. Nakiboğlu, O. Rudenko, A. Hirschberg, Aeroacoustics of the swinging corrugated tube: Voice of the dragon, J. Acoust. Soc. Am. 131 (1) (2012) 749–765.

[11] S. C. Belfroid, D. P. Shatto, M. Peters, Flow induced pulsations caused by corrugated tubes, in: ASME Pressure, Vessels and Piping Conference, San Antonio, TX, 2007.

[12] J. Golliard, N. González-Díez, S. Belfroid, G. Nakiboğlu, A. Hirschberg, U-RANS model for the prediction of the acoustic sound power generated in a whistling corrugated pipe, in: ASME. Pressure Vessels and Piping Conference, Paris, France, 2013.

[13] G. Nakiboğlu, A. Hirschberg, Aeroacoustic power generated by multiple compact axisymmetric cavities: Effect of hydrodynamic interference on the sound production, Phys. Fluids 24 (6) (2012) 067101.

[14] A. A. Shaaban, S. Ziada, Acoustic response of multiple shallow cavities and prediction of self-excited acoustic oscillations, J. Fluids Eng. 140 (9) (2018).

[15] A. A. Shaaban, S. Ziada, Fully developed building unit cavity source for long multiple shallow cavity configurations, Phys. Fluids 30 (8) (2018) 086105.

[16] O. Rudenko, G. Nakiboğlu, A. Holten, A. Hirschberg, On whistling of pipes with a corrugated segment: Experiment and theory, J. Sound Vib. 332 (26) (2013) 7226–7242.

[17] J. Golliard, S. Belfroid, O. Vijlbrief, K. Lunde, Direct measurements of acoustic damping and sound amplification in corrugated pipes with flow, in: ASME. Pressure Vessels and Piping Conference, Boston, MA, 2015.

[18] J. Golliard, F. Sanna, D. Violato, Y. Auregan, Measured source term in corrugated pipes with flow. effect of diameter on pulsation source, in: 22nd AIAA/CEAS Aeroacoustics Conference, 2016, Lyon, France, 2016.

[19] S. Belfroid, N. González Díez, J. Golliard, K. Lunde, S. Naess, Damping and source strength characteristics of corrugated pipes: influence gap width, in: 9th International Symposium on Fluid-Structure Interactions, Flow-Sound Interactions, Flow-Induced Vibration & Noise, 2018.

[20] Y. Aurégan, R. Starobinski, Determination of acoustical energy dissipation / production potentiality from the acoustical transfer functions of a multiport, Acta Acust. 85 (1999) 788–792.

[21] P. Testud, Y. Aurégan, P. Moussou, A. Hirschberg, The whistling potentiality of an orifice in a confined flow using an energetic criterion, J. Sound Vib. 325 (4) (2009) 769–780.

[22] R. Lacombe, P. Moussou, Y. Aurégan, Whistling of an orifice in a reverberating duct at low mach number, J. Acoust. Soc. Am. 130 (5) (2011) 2662–2672.

[23] Y. Aurégan, V. Pagneux, $\mathcal{PT}$-symmetric scattering in flow duct acoustics, Phys. Rev. Lett. 118 (2017) 174301.

[24] M. Karlsson, M. Åbom, On the use of linear acoustic multiports to predict whistling in confined flows, Acta Acust. 97 (1) (2011) 24–33.

[25] Y. Aurégan, M. Leroux, Failures in the discrete models for flow duct with perforations: an experimental investigation, J. Sound Vib. 265 (1) (2003) 109–121.

[26] Y. Aurégan, V. Pagneux, Slow sound in lined flow ducts, J. Acoust. Soc. Am. 138 (2) (2015) 605–613.

[27] H. Schlichting, Boundary-layer theory, McGraw-Hill, 1979.

[28] G. Kooijman, A. Hirschberg, J. Golliard, Acoustical response of orifices under grazing flow: Effect of boundary layer profile and edge geometry, J. Sound Vib. 315 (2008) 849–874.